

# Many-Body Dispersion Interactions in Molecular Crystal Polymorphism\*\*

Noa Marom,\* Robert A. DiStasio Jr., Viktor Atalla, Sergey Levchenko, Anthony M. Reilly, James R. Chelikowsky, Leslie Leiserowitz, and Alexandre Tkatchenko\*

Polymorphs of molecular crystals are often very close in energy, yet they may possess very different physical and chemical properties. The understanding of polymorphism is therefore of great importance for a variety of applications, ranging from drug design to nonlinear optics and hydrogen storage.<sup>[1–3]</sup> While the crystal structure prediction blind tests conducted by the Cambridge Crystallographic Data Centre have shown steady progress toward reliable structure prediction for molecular crystals,<sup>[4]</sup> several challenges remain, including molecular salts, hydrates, and flexible molecules with several stable conformers. The ability to identify and rank all of the relevant polymorphs of a given molecular crystal hinges on an accurate description of their relative energetic stability. Hence, a first-principles quantum mechanical method that can attain the required accuracy of around 0.1–0.2 kcal mol<sup>−1</sup> would clearly be an indispensable tool for polymorph prediction. In this work, we show that accounting for the nonadditive many-body dispersion (MBD) energy beyond the standard pairwise approximation is crucial for the correct qualitative and quantitative description of polymorphism in molecular crystals. We demonstrate this through

three fundamental and stringent benchmark examples: glycine, oxalic acid, and tetrolic acid. These systems represent a broad class of molecular crystals, comprising hydrogen-bonded (H-bonded) networks of amino acids and carboxylic acids.

Among the first-principles methods, density functional theory (DFT) is the most widely used approach in the study of polymorphism in molecular crystals. However, most common exchange-correlation functionals (including hybrid functionals) are based on semi-local electron correlation, and thereby fail to capture the contribution of dispersion interactions to the stability of molecular crystals. These ubiquitous non-covalent interactions are quantum mechanical in nature and correspond to the multipole moments induced in response to instantaneous fluctuations in the electron density. To incorporate these long-range electron correlation effects within DFT, significant progress has been made by using the standard  $C_6/R^6$  pairwise additive expression for the dispersion energy.<sup>[5–7]</sup> Indeed, DFT with pairwise dispersion terms can yield accurate results when the energy differences between molecular crystal polymorphs are sufficiently large.<sup>[8–10]</sup> Notably, Neumann et al. have achieved the highest success rate in the last two blind tests using such methods.<sup>[4,11]</sup> However, these pairwise dispersion approaches, even when used in conjunction with state-of-the-art functionals, are still unable to reach the level of accuracy required to describe polymorphism in many relevant molecular crystals, including glycine and oxalic acid.<sup>[12–17]</sup>

Recently, a novel and efficient method for describing the many-body dispersion (MBD) energy has been developed,<sup>[18]</sup> building upon the Tkatchenko–Scheffler (TS) pairwise method.<sup>[19]</sup> Within the TS approach, the effective dispersion coefficients ( $C_6$ ) are calculated from the DFT electron density, hence the effect of the local environment of an atom in a molecule is accurately accounted for by construction. The MBD method presents a two-fold improvement over the TS approach by including: 1) the long-range electrodynamic screening through the self-consistent solution of the dipole–dipole electric-field coupling equations for the effective polarizability, and 2) the non-pairwise-additive many-body dispersion energy to infinite order through diagonalization of the Hamiltonian corresponding to a system of coupled fluctuating dipoles. The inclusion of the MBD energy in DFT leads to a significant improvement in the binding energies between organic molecules,<sup>[18,21]</sup> and for the cohesion of the benzene and oligoacene molecular crystals.<sup>[18,21]</sup> The MBD energy, like the TS energy, can be added to any DFT functional, requiring only the adjustment of a single range-separation parameter per functional.<sup>[18,19]</sup>

[\*] N. Marom, J. R. Chelikowsky  
Center for Computational Materials  
Institute for Computational Engineering and Sciences  
The University of Texas at Austin  
Austin, TX 78712 (USA)  
E-mail: noa@ices.utexas.edu

R. A. DiStasio Jr.  
Department of Chemistry, Princeton University  
Princeton, NJ 08544 (USA)

V. Atalla, S. Levchenko, A. M. Reilly, A. Tkatchenko  
Fritz-Haber-Institut der Max-Planck-Gesellschaft  
Faradayweg 4–6, 14195 Berlin (Germany)  
E-mail: tkatchen@fhi-berlin.mpg.de

L. Leiserowitz  
Department of Materials and Interfaces  
Weizmann Institute of Science  
Rehovoth 76100 (Israel)

[\*\*] A.T. acknowledges support from ERC Starting Grant VDW-CMAT. N.M. and J.R.C. acknowledge support from the Scientific Discovery through Advanced Computing (SciDAC) program funded by the U.S. Department of Energy, Office of Science, Advanced Scientific Computing Research and Basic Energy Sciences under award number DESC0008877. This research used resources of the Argonne Leadership Computing Facility at Argonne National Laboratory, which is supported by the Office of Science of the U.S. DOE under contract number DE-AC02-06CH11357. We thank J. F. Hammond and O. A. von Lilienfeld from ALCF for their support.

Supporting information for this article is available on the WWW under <http://dx.doi.org/10.1002/anie.201301938>.

We begin with a detailed analysis of the glycine (Gly) molecular crystal, which has three experimentally observed polymorphs:  $\alpha$ -Gly,  $\beta$ -Gly, and  $\gamma$ -Gly, as illustrated in Figure 1. Figure 2 shows the performance of different DFT

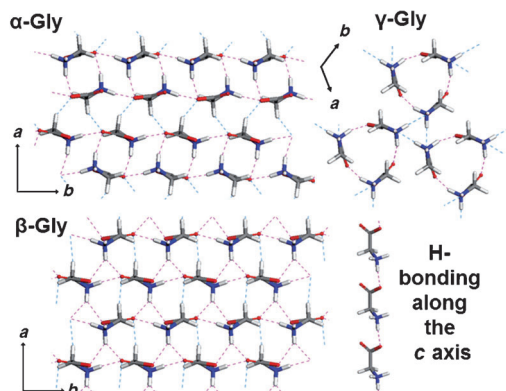


**Figure 1.** Structures of the three polymorphs of glycine. H-bonds are indicated by dashed lines. The translation-related H-bonded chain along the  $c$  axis, common to all three polymorphs, is also shown.

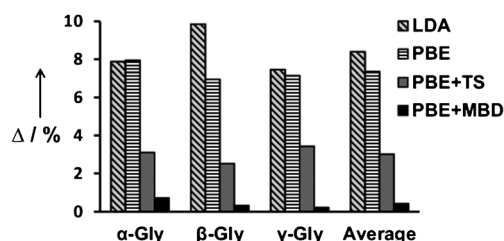


**Figure 2.** Absolute percent error  $\Delta$  in the calculated unit cell volumes of the glycine polymorphs with respect to low-temperature experiments ( $\alpha$ -Gly: Refs. [26, 27],  $\beta$ -Gly: Ref. [28],  $\gamma$ -Gly: Ref. [29]). The LDA and PBE data were taken from Ref. [22]. Note that LDA underestimates the unit cell volumes, while PBE overestimates them.

methods for the calculation of the unit cell volumes of these glycine polymorphs with respect to low-temperature experiments. A complete account of the computational details and cell parameters obtained with the different methods is provided in the Supporting Information. As shown in

Ref. [22], the local-density approximation (LDA)<sup>[23]</sup> underestimates the unit cell volumes by 7–10%, while the generalized-gradient approximation of Perdew, Burke, and Ernzerhof (PBE)<sup>[24, 25]</sup> overestimates the unit cell volumes by 7–8%.<sup>[22]</sup> Adding the pairwise TS energy to the PBE functional reduces the error in the unit cell volumes to about 3%, a significant improvement. PBE + MBD yields a further noticeable improvement with an accuracy of 0.3% for the unit cell volumes of  $\beta$ -Gly and  $\gamma$ -Gly and 0.8% for  $\alpha$ -Gly.

Both  $\alpha$ -Gly and  $\beta$ -Gly consist of H-bonded sheets of glycine in the  $a$ - $c$  plane. The strong H-bonds within the glycine sheets (shown in magenta in Figure 1), are described reasonably well by PBE even without accounting for dispersion interactions. This is not the case for the weaker interactions between the glycine sheets, along the  $b$  direction (shown in light blue in Figure 1). For  $\beta$ -Gly, where the glycine sheets are bound by bifurcated  $\text{NH}\cdots\text{O}$  bonds, PBE overestimates  $b$  by 5%. PBE + TS reduces this overestimation to 1% and PBE + MBD yields excellent agreement with experiment. In  $\alpha$ -Gly, the glycine sheets form a H-bonded ( $\text{NH}\cdots\text{O}$ ) bilayer, through the centers of inversion. The three-dimensional (3D) network is then completed by weaker  $\text{CH}\cdots\text{O}$  interactions between the bilayers. These interactions determine the direction of the glide as well as the inter-bilayer distance along the  $b$  axis. The weak interactions along the  $b$  direction are reflected by a significant temperature dependence of the  $b$  parameter of  $\alpha$ -Gly.<sup>[27, 30]</sup> PBE grossly overestimates  $b$  by 0.65 Å. The overestimation is significantly reduced to 0.16 Å at the PBE + TS level of theory. For the  $b$  parameter of  $\alpha$ -Gly, PBE + MBD does not yield further improvement over PBE + TS because the potential energy surface is very flat—the binding energy changes by only 0.01 eV per unit cell for 11.75 Å <  $b$  < 12.15 Å.

The most stable  $\gamma$ -Gly polymorph has the same translation-related H-bonded chain motif as  $\alpha$ -Gly and  $\beta$ -Gly along the  $c$  axis. However, it is different because the H-bonded chains form helices, related by three-fold screw symmetry, rather than sheets. The helices are held together by lateral  $\text{NH}\cdots\text{O}$  H bonds, forming a 3D network. The inter-helix H-bonds (shown in light blue in Figure 1) are longer than the intra-helix H-bonds (shown in magenta in Figure 1). The  $c$  parameter is reproduced correctly even by PBE, however, the  $a$  and  $b$  parameters are significantly improved by including dispersion interactions. Figure 3 shows the

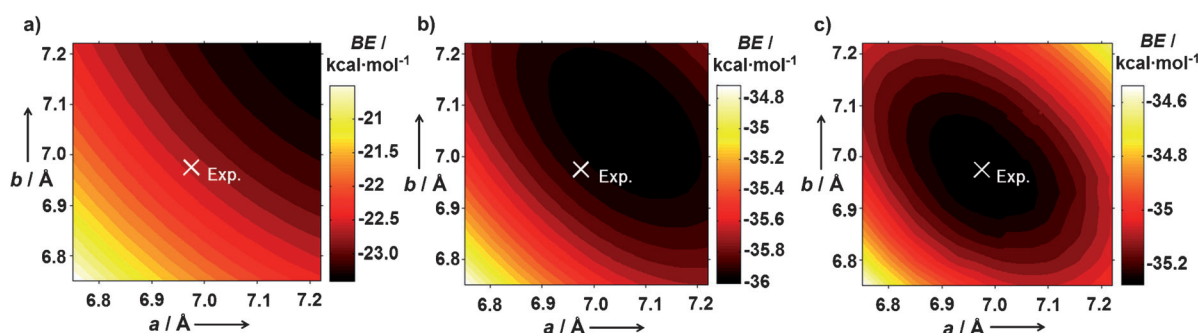


**Figure 3.** Potential-energy surfaces for the  $a$ - $b$  plane of  $\gamma$ -Gly,<sup>[31]</sup> obtained using: a) PBE, b) PBE + TS, and c) PBE + MBD. Experimental lattice parameters are marked by a cross.<sup>[22]</sup> The experimental error bars are not visible on this scale ( $BE$  = binding energy).

change of the potential-energy landscape in the  $a$ - $b$  plane of  $\gamma$ -Gly (with  $c$  fixed at 5.48 Å), with different levels of approximation for the dispersion contributions. The pairwise TS method significantly increases the binding energy ( $BE$ ) and improves the position of the minimum, as compared to PBE. However, it is still insufficient for obtaining the correct experimental geometry. Accounting for the MBD interactions correctly captures the weak and complex inter-helix interactions, leading to a slight decrease in the crystal binding energy and a minimum in excellent agreement with experiment.

We now discuss the relative stability of the glycine polymorphs. Experimentally, it is known that  $\gamma$ -Gly is the most stable polymorph,<sup>[30]</sup> although the energy difference between  $\gamma$ -Gly and  $\alpha$ -Gly is very small. It is also well known that  $\beta$ -Gly is less stable than both  $\gamma$ -Gly and  $\alpha$ -Gly.<sup>[35]</sup> The calculated relative energies, including the zero-point energy (ZPE), are shown in Figure 4 and compared to the exper-

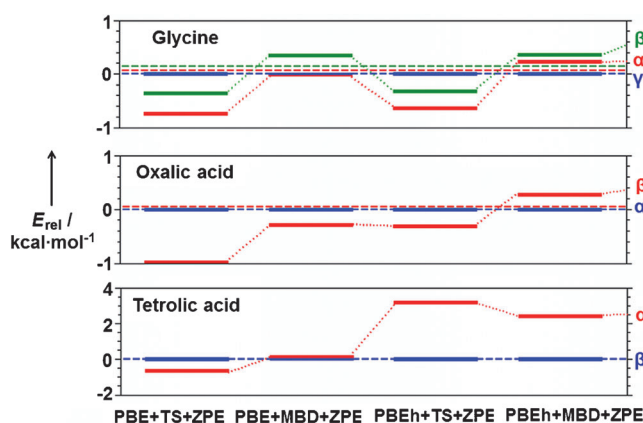


**Figure 4.** Computed relative stabilities of the polymorphs of glycine (top), oxalic acid (middle), and tetrolic acid (bottom). Experimental data from Refs. [30, 32–34] are shown as dashed lines.

imentally determined relative enthalpies from Refs. [30, 32]. Tabulated values are given in the Supporting Information. The PBE + TS method yields the wrong order of stability:  $\alpha > \beta > \gamma$ , and the energy differences between the polymorphs are overestimated. Similar overestabilization of the  $\alpha$  form has been reported for a different pairwise dispersion method.<sup>[16]</sup> Including the many-body dispersion effects through the PBE + MBD method significantly improves the agreement with experiment. In this case, the  $\alpha$  and  $\gamma$  forms are nearly degenerate, with the  $\beta$  form somewhat less stable, and the energy differences are also much closer to experiment. The PBE-based hybrid functional (PBEh), which includes 25% exact exchange, has been shown to provide a more reliable description of hydrogen bonds<sup>[36]</sup> and short-range vdW interactions<sup>[37]</sup> than PBE. Indeed, PBEh + MBD further improves upon the relative stability of the three polymorphs of glycine as shown in Figure 4, yielding the correct order of stability:  $\gamma > \alpha > \beta$ .

The importance of MBD interactions is also seen for the polymorphs of oxalic and tetrolic acid, shown in Figure 5.

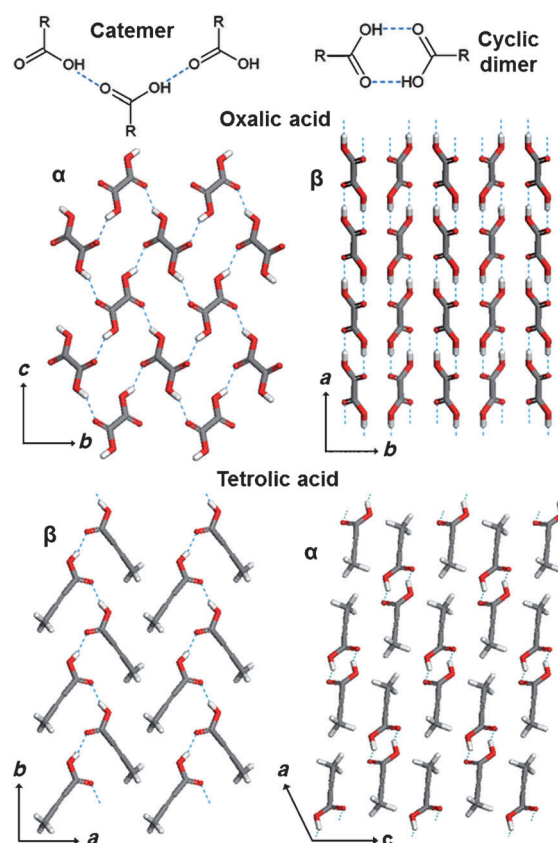


**Figure 5.** Structures of the polymorphs of oxalic and tetrolic acid. H bonds are indicated by dashed lines.

Carboxylic acids have two modes of interlinking via OH...O hydrogen bonds: a cyclic dimer, as in  $\beta$ -oxalic and  $\alpha$ -tetrolic acid, and a catemer, as in  $\alpha$ -oxalic and  $\beta$ -tetrolic acid.<sup>[38]</sup> In both cases, the catemer structure is known to be more stable.<sup>[33, 34, 39]</sup> For oxalic acid, the enthalpies of sublimation of both polymorphs have been measured at room temperature.<sup>[33, 34]</sup> These measured enthalpies may be converted to a lattice energy difference of 0.05 kcal mol<sup>−1</sup> (shown as dashed lines in Figure 4) by using the PBE + TS vibrational quantities in the harmonic approximation.<sup>[40]</sup> The computed energy differences obtained using the PBE and PBEh functionals combined with the TS and MBD dispersion methods are shown in Figure 4, while tabulated values are given in the Supporting Information. For both oxalic and tetrolic acid, PBE + TS overestabilizes the cyclic dimer with respect to the catemer, yielding the wrong order of stability of the polymorphs. Similar overestabilization of the  $\beta$  polymorph of oxalic acid has been seen for other pairwise methods.<sup>[17]</sup> The inclusion of exact exchange, through the PBEh functional, and the inclusion of MBD interactions both contribute to the stabilization of the catemer with respect to the cyclic dimer. For oxalic acid, as for glycine, only PBEh + MBD produces the correct energetic ordering of the polymorphs with  $\alpha$  being more stable than  $\beta$ . For tetrolic acid, PBE + MBD already makes the catemer-based  $\beta$  form slightly more stable than the cyclic dimer-based  $\alpha$  form and PBEh + MBD increases the energy difference between the two forms.

In summary, we have demonstrated that an accurate description of the nonadditive many-body dispersion energy with the DFT+MBD method reproduces the energetic ordering of polymorphs for three different molecular crystals, glycine, oxalic acid, and tetrolic acid, when compared to reliable experimental results. The improvement obtained with the MBD method as compared to the simple pairwise dispersion model is attributed to the sensitive dependence of the dispersion energy on the polymorph geometry and the dynamic internal electric fields produced in molecular crystals. The DFT+MBD method yields an unprecedented accuracy of 1% in the description of the structures of molecular crystal polymorphs and of 0.2 kcal mol<sup>-1</sup> in their relative energies. Such accuracy is essential for the reliable modeling of polymorphism in molecular crystals.

Received: March 7, 2013

Published online: May 16, 2013

**Keywords:** ab initio calculations · dispersion interactions · intermolecular interactions · molecular crystals · polymorphism

- [1] J. Bernstein in *Polymorphism in Molecular Crystals*, Oxford University Press, New York, **2002**.
- [2] S. L. Price, *Phys. Chem. Chem. Phys.* **2008**, *10*, 1996.
- [3] S. L. Price, *Acc. Chem. Res.* **2009**, *42*, 117.
- [4] D. A. Bardwell, C. S. Adjiman, Y. A. Arnautova, E. Bartashevich, S. X. M. Boerrigter, D. E. Braun, A. J. Cruz-Cabeza, G. M. Day, R. G. Della Valle, G. R. Desiraju, B. P. van Eijck, J. C. Facelli, M. B. Ferraro, D. Grillo, M. Habgood, D. W. M. Hofmann, F. Hofmann, K. V. Jovan Jose, P. G. Karamertzanis, A. V. Kazantsev, J. Kendrick, L. N. Kuleshova, F. J. J. Leusen, A. V. Maleev, A. J. Misquitta, S. Mohamed, R. J. Needs, M. A. Neumann, D. Nikylov, A. M. Orendt, R. Pal, C. C. Pantelides, C. J. Pickard, L. S. Price, S. L. Price, H. A. Scheraga, J. van de Sreek, T. S. Thakur, S. Tiwari, E. Venuti, I. K. Zhitkov, *Acta Crystallogr. Sect. B* **2011**, *67*, 535.
- [5] K. E. Riley, M. Pitonak, P. Jurecka, P. Hobza, *Chem. Rev.* **2010**, *110*, 5023.
- [6] S. Grimme, *Comput. Mol. Sci.* **2011**, *1*, 211.
- [7] N. Marom, A. Tkatchenko, M. Rossi, V. V. Gobre, O. Hod, M. Scheffler, L. Kronik, *J. Chem. Theory Comput.* **2011**, *7*, 3944.
- [8] H. C. S. Chan, J. Kendrick, F. J. J. Leusen, *Phys. Chem. Chem. Phys.* **2011**, *13*, 20361.
- [9] N. Marom, A. Tkatchenko, S. Kapishnikov, L. Kronik, L. Leiserowitz, *Cryst. Growth Des.* **2011**, *11*, 3332.
- [10] B. Schatschneider, J.-J. Liang, S. Jezowski, A. Tkatchenko, *CrystEngComm* **2012**, *14*, 4656.
- [11] M. A. Neumann, F. J. J. Leusen, J. Kendrick, *Angew. Chem.* **2008**, *120*, 2461; *Angew. Chem. Int. Ed.* **2008**, *47*, 2427.
- [12] G. J. O. Beran, K. Nanda, *J. Phys. Chem. Lett.* **2010**, *1*, 3480.
- [13] K. Hongo, M. A. Watson, R. S. Sanchez-Carrera, T. Iitaka, A. Aspuru-Guzik, *J. Phys. Chem. Lett.* **2010**, *1*, 1789.
- [14] O. A. von Lilienfeld, A. Tkatchenko, *J. Chem. Phys.* **2010**, *132*, 234109.
- [15] S. Wen, K. Nanda, Y. Huang, G. Beran, *Phys. Chem. Chem. Phys.* **2012**, *14*, 7578.
- [16] Q. Zhu, A. R. Oganov, C. W. Glass, H. T. Stokes, *Acta Crystallogr. Sect. B* **2012**, *68*, 215.
- [17] A. Otero-de-la-Roza, E. R. Johnson, *J. Chem. Phys.* **2012**, *137*, 054103.
- [18] A. Tkatchenko, R. A. DiStasio, Jr., R. Car, M. Scheffler, *Phys. Rev. Lett.* **2012**, *108*, 236402.
- [19] A. Tkatchenko, M. Scheffler, *Phys. Rev. Lett.* **2009**, *102*, 073005.
- [20] R. A. DiStasio, Jr., O. A. von Lilienfeld, A. Tkatchenko, *Proc. Natl. Acad. Sci. USA* **2012**, *109*, 14791–14795.
- [21] B. Schatschneider, J.-J. Liang, A. M. Reilly, N. Marom, G.-X. Zhang, A. Tkatchenko, *Phys. Rev. B* **2013**, *87*, 060104.
- [22] J. A. Chisholm, S. Motherwell, P. R. Tulip, S. Parsons, S. J. Clark, *Cryst. Growth Des.* **2005**, *5*, 1437.
- [23] J. P. Perdew, Y. Wang, *Phys. Rev. B* **1992**, *45*, 13244.
- [24] J. P. Perdew, K. Burke, M. Ernzerhof, *Phys. Rev. Lett.* **1996**, *77*, 3865.
- [25] J. P. Perdew, K. Burke, M. Ernzerhof, *Phys. Rev. Lett.* **1997**, *78*, 1396.
- [26] J. Netzel, A. Hofmann, S. van Smaalen, *CrystEngComm* **2008**, *44*, 3226.
- [27] R. Destro, P. Roversi, M. Barzaghi, R. E. Marsh, *J. Phys. Chem. A* **2000**, *104*, 1047.
- [28] E. V. Boldyreva, T. N. Drebuschak, E. S. Shutova, *Z. Kristallogr.* **2003**, *218*, 366.
- [29] A. Kvick, W. M. Canning, T. F. Koetzle, G. J. B. Williams, *Acta Crystallogr. Sect. B* **1980**, *36*, 115.
- [30] G. L. Perlovich, L. K. Hansen, A. Bauer-Brandl, *J. Therm. Anal.* **2001**, *66*, 699.
- [31] The binding energy per unit cell is referenced to a glycine zwitterion.
- [32] We assume that the solvation enthalpy of the three polymorphs in water is approximately equal, so that the measured differences between the solution enthalpies are directly comparable to total energy differences.
- [33] H. G. M. de Wit, J. A. Bouwstra, J. G. Blok, C. G. de Kruif, *J. Chem. Phys.* **1983**, *78*, 1470.
- [34] R. S. Bradley, S. Cotson, *J. Chem. Soc.* **1953**, 1684.
- [35] I. Weissbuch, V. Y. Torbeev, L. Leiserowitz, M. Lahav, *Angew. Chem.* **2005**, *117*, 3290; *Angew. Chem. Int. Ed.* **2005**, *44*, 3226.
- [36] B. Santra, J. Klimes, D. Alfe, A. Tkatchenko, B. Slater, A. Michaelides, R. Car, M. Scheffler, *Phys. Rev. Lett.* **2011**, *107*, 185701.
- [37] A. Tkatchenko, O. A. von Lilienfeld, *Phys. Rev. B* **2008**, *78*, 045116.
- [38] L. Leiserowitz, *Acta Crystallogr. Sect. B* **1976**, *32*, 775.
- [39] V. Benghiat, L. Leiserowitz, *J. Chem. Soc. Perkin Trans. 2* **1972**, 1763.
- [40] A. M. Reilly, A. Tkatchenko, *J. Phys. Chem. Lett.* **2013**, *4*, 1028–1033.